Ethiopian Journal of Science and Sustainable Development

e-ISSN 2663-3205 *Volume 9 (2), 2022*

Journal Home Page: www.ejssd.astu.edu.et

Research Paper

Estimation of Relativistic Mass Correction for Electronic and Muonic Hydrogen Atoms with Potential from Finite Size Source

Eshetu Diriba Kena*, Gashaw Bekele Adera

Haramaya University, Department of Physics, P.O.Box 138, Dire Dawa, Ethiopia

Article Info

Article History:
Received 25 April 2022
Received in revised form 26 July 2022
Accepted 28 July 2022

Keywords:
Atomic structure
Charge distributions
Finite size source
Hydrogen-like atom
Muonic hydrogen
Point-like source
Relativistic mass correction

Abstract

Hydrogen is the simplest atom in nature which helps us to study fundamental properties and structure of atoms. In this work, the perturbed Schrodinger equation is used to estimate relativistic mass correction with potentials from finite size sources. This study is done with the assumption that the changes in both energy eigenvalues and eigenfunctions are negligible when considering the finite size of the nuclei. The relativistic mass corrections to 1s 1/2 and 2s_1/2 states using potential from finite size source are obtained and compared with corrections using potential from point-like source. The results show that, for hydrogen-like atoms with light nuclei the relativistic mass corrections due to the finite size source roughly coincides with that of point-like source. However, for atoms with heavy nuclei the two corrections display strong disagreement in which the corrections with finite size nuclei are significantly smaller than that of point-like nuclei. Thus, this study offers the first attempt at including relativistic mass correction to energy eigenvalues of electronic and muonic hydrogen-like atoms with finite-size nuclei. When experimental data become available, comparison of these theoretical predictions may give a better insight into how relativistic corrections are affected by finite-size nuclei.

1. Introduction

The hydrogen atom is the simplest atom known to exist in nature, which makes it very suitable to study the fundamental properties and structure of atoms. The hydrogen atom consists of a single negatively charged electron that moves about a positively charged proton (Hudson and Nelson, 1990, Adamu et al., 2018). In 1911, Niels Bohr introduced the first model of hydrogen atom based on Planck's hypothesis, which states that electromagnetic radiations can only be emitted or absorbed in quanta of energy. However, the complete understanding of the structure of atomic elements in the periodic table was made possible with the invention of new theory called quantum mechanics as of 1925 (Beiser, 2003)

In addition, recent studies show that it is possible to replace the electron in an atom by a muon to form muonic atom. In other words, Muonic hydrogen is an atom consisting of the proton and the muon which is very similar to the well-known electronic hydrogen (Pohl et al., 2013). As a result, theoretical descriptions of the two atomic types have many features in common. The main difference however, is the fact that the muon mass is about 207 times heavier than that of the electron. The massiveness of muon in turn results in a significant increase in the energy levels of the atoms (Pohl, 2014 and Patoary et al., 2018); and leads to the realization that muons tend to be close to the nucleus of an atom as

E-mail: eshetudiriba444@gmail.com

https://doi.org/10.20372/ejssdastu:v9.i2.2022.474

compared to electrons in electronic hydrogen (Eshetu Diriba and Gashaw Bekele, 2021).

In a simplest quantum description of hydrogen atom, its nucleus is assumed to be point-like in terms of its mass and charge distribution. Nevertheless, the more realistic model treats the nucleus as having finite size distributions. The shift in energy eigenvalues and eigenfunctions due to the finite size nucleus of muonic hydrogen atom has been studied non-relativistically using perturbation theory (Adamu and Ngadda, 2017). But in relativistic framework, the Dirac equation of bound muon can be solved exactly or using relativistic perturbation (Niri and Anjami, 2018, Firew Meka, 2020, Adamu and Ngadda, 2017, Deck et al., 2005 and Eshetu Diriba and Gashaw Bekele, 2021). It is worth noting that the relativistic effects play key role in the studies of the molecular properties such as electron affinities, ionization potentials, reaction, dissociation energies, spectroscopic and other properties (Iliaš et al., 2010 and Pyper, 2020). The relativistic effects can also be used to investigate the rotation curve of disk galaxies which is significant at large radii (Deur, 2021).

In non-relativistic treatment of an atom, the standard Schrodinger equation conveys only a limited amount of information about properties of the atom. For instance, consideration of relativistic effects such as relativistic mass correction, spin-orbit coupling and Darwin terms, leads to a better description of atoms and their structure. Traditionally, those corrections are taken into account for hydrogen-like atoms with Coulomb potential from a point-like source (Schwabl, 2008 and Townsend, 2012). To the best of our knowledge, however, no work has been done that examines relativistic effects for those atoms with Coulomb potential from a finite size source. According to Ref. (Niri and Anjami, 2018 and Deck et al., 2005), the corrections to energy eigenvalues due to finite size nucleus for muonic hydrogen in non-relativistic treatment are negligibly small; and the same can be said for corrections to energy eigenfunctions.

In this paper, the Schrodinger equation has been revisited as an attempt to address the relativistic mass correction to electronic and muonic hydrogen-like atoms by replacing the point-like potential source with Coulomb potential from finite size source. This is done so with the assumption that such replacement may not result in any significant shifts in both energy eigenvalues and eigenstates. Finally, the results of this work are compared with those obtained for hydrogen-like atoms with point-like source charge for light and heavy atomic nuclei.

2. Mathematical methodology

In this chapter we are going to introduce the mathematical methodology and methods needed to achieve our research objectives

2.1. Dirac Equation: Minimal Coupling

Dirac equation for a particles in an electromagnetic field, A_μ, is modified as

$$[\gamma^\mu i\partial_\mu - mI]\Psi = 0 \quad \longrightarrow \quad [\gamma^\mu(i\partial_\mu - eA_\mu) - mI]\Psi = 0 \qquad (1)$$

More explicitly Eq. (1) can be written as

$$[\gamma^0 i\partial_0 - eA_0 + \vec{\gamma}\cdot(i\vec{\nabla} + e\vec{A}) - mI]\Psi = 0 \qquad (2)$$

where,

$$\gamma^0 = \begin{pmatrix} I & 0 \\ 0 & -I \end{pmatrix},\ \vec{\gamma} = \begin{pmatrix} o & \vec{\sigma} \\ -\vec{\sigma} & 0 \end{pmatrix},\ I = \begin{pmatrix} 1 & 0 \\ 0 & 1 \end{pmatrix}$$

2.2. Algebra of Gamma Matrices

2.2.1. Pauli matrices

The Pauli matrices are a set of 2×2 complex, Hermitian, and unitary matrices

$$\sigma_x = \begin{pmatrix} 0 & 1 \\ 1 & 0 \end{pmatrix},\ \sigma_y = \begin{pmatrix} 0 & -i \\ i & 0 \end{pmatrix},\ \sigma_z = \begin{pmatrix} 1 & 0 \\ 0 & -1 \end{pmatrix} \qquad (3)$$

Using the commutation and anti-commutation relation of Pauli matrices we obtain

$$\sigma_i\sigma_j = \delta_{ij} + i\sum\epsilon_{ijk}\sigma_k \qquad (4)$$

Equation 4 helps us to prove the relation

$$(\vec{\sigma}\cdot\vec{\mathrm{A}})(\vec{\sigma}\cdot\vec{B}) = \vec{A}\cdot\vec{B} + i\vec{\sigma}\cdot(\vec{A}\times\vec{B}) \qquad (5)$$

2.3. Numerical Calculation of Calculation of Relativistic Mass correction

We employ MATLAB 2013a software to numerically generate relativistic mass correction. Finally, we plot the graph of electronic and muonic hydrogen atoms as a function of proton number.

3. Formalism

In this section, we cover the mathematical origin of relativistic effects and then derive relativistic mass corrections for hydrogen-like atoms with potential from point-like and finite size sources. In this work, we invoke the natural unit whereby we set $\hbar = c = 1$.

3.1. Reduction of Dirac Equation into Non-relativistic Equation

In the presence of a spherically symmetric electromagnetic potential the Dirac equation takes the form

$$H\psi = (\vec{\alpha}\cdot\vec{\pi} + \beta m + V(r))\psi, \tag{6}$$

where, the kinematic momentum operator is given in terms of vector potential $\vec{A}$ as

$$\vec{\pi} = \vec{p} - e\vec{A} \tag{7}$$

The four parameters $\vec{\alpha}$ and β are written in block matrix format using Pauli and identity matrices:

$$\vec{\alpha} = \begin{pmatrix} 0 & \vec{\sigma} \\ \vec{\sigma} & 0 \end{pmatrix}; \qquad \beta = \begin{pmatrix} 1 & 0 \\ 0 & -1 \end{pmatrix} \tag{8}$$

Let's redefine the Dirac spinor ψ, which is a four dimensional column vector as

$$\psi = \begin{pmatrix} \phi \\ \chi \end{pmatrix} \tag{9}$$

Substituting Eqs. (6) - (9) into Eq. (6) gives

$$(E - m - V)\phi = \vec{\sigma}\cdot\vec{\pi}\chi \tag{10}$$

$$(E + m - V)\chi = \vec{\sigma}\cdot\vec{\pi}\phi \tag{11}$$

In non-relativistic limit, we relate the relativistic and non-relativistic energies as (Townsend, 2012 and Maggiore, 2005)

$$E_{NRT} = E - m \tag{12}$$

Plugging Eq. (12) into Eqs. (10) and (11) yields

$$(E_{NRT} - V)\phi = i\vec{\sigma}\cdot\vec{\pi}\chi \tag{13}$$

$$(E_{NRT} + 2m - V)\chi = \vec{\sigma}\cdot\vec{\pi}\phi \tag{14}$$

The non-relativistic energy E_{NRT} and the potential V terms are very small in comparison with $2m$ and are therefore neglected (Messiah, 1966). Hence Eq. (14) is approximated as

$$\chi = \frac{\vec{\sigma}\cdot\vec{\pi}}{2m}\phi \tag{15}$$

Inserting Eq. (15) back into Eq. (13) and we get

$$E_{NRT}\phi = \left[\frac{1}{2m}(\vec{\sigma}\cdot\vec{\pi})(\vec{\sigma}\cdot\vec{\pi}) + eA_0\right]\phi, \tag{16}$$

where, the potential energy V has been expressed in terms of scalar potential$A_0 (V = eA_0)$. By using the property of Pauli matrices, we may write

$$(\vec{\sigma}\cdot\vec{\pi})(\vec{\sigma}\cdot\vec{\pi}) = \vec{\pi}^2 + i\vec{\sigma}\cdot(\vec{\pi}\times\vec{\pi}) = \vec{\pi}^2 - e\vec{\sigma}\cdot\vec{B},$$

which in turn allows us to re-express Eq. (16) as

$$E_{NRT}\phi = \left[\frac{(\vec{p} - e\vec{A})^2}{2m} - \frac{e\vec{\sigma}\cdot\vec{B}}{2m} + eA_0\right]\phi. \tag{17}$$

The expression in Eq. (17) is famously known as the Pauli equation. This Pauli equation can further be manipulated to become the non-relativistic Schrodinger equation which naturally incorporate all relativistic corrections and appropriate for spin-half particles (Maggiore, 2005):

$$E_{NRT}\phi = \left[\frac{p^2}{2m} + V - \frac{p^4}{8m^3} + \frac{1}{2m^2}\frac{1}{r}\frac{dV}{dr}\vec{S}\cdot\vec{L} - \frac{e}{8m^2}\vec{\nabla}\cdot\vec{E}\right]\phi, \tag{18}$$

where, $-p^4/8m^3$ is the relativistic mass correction, the term $\vec{S}\cdot\vec{L}$ is spin-orbit coupling and $\vec{\nabla}\cdot\vec{E}$ is the Darwin term.

3.2. Relativistic mass correction for point-like source

Relativistic mass correction is often referred as kinetic energy correction, which can also be obtained from energy-momentum relation for relativistic particle in the limit $|\vec{p}| \ll m$. As we can see from Eq. (13) the perturbed Hamiltonian due to relativistic mass correction is given by

$$\hat{H}_1 = -\frac{p^4}{8m^3} \tag{19}$$

The Hamiltonian of unperturbed system is given by

$$H_0 = \frac{p^2}{2m} + V$$

Squaring both sides and rearranging give rise to

$$\frac{p^4}{8m^3} = \frac{1}{2m}(H_0 - V)^2 \tag{20}$$

By using Eq. (20), we may rewrite Eq. (19) as

$$\hat{H}_1 = -\frac{1}{2m}(H_0 - V)^2 \tag{21}$$

The relativistic mass correction to energy levels of hydrogen atom can be written as (Griffiths, 1995)

$$\Delta E_1^{(n)} = \langle\psi_{nlm}|\hat{H}_1|\psi_{nlm}\rangle \tag{22}$$

Putting Eq. (21) into the above equation we obtain

$$\Delta E_1^{(n)} = -\frac{1}{2m}\langle\psi_{nlm}|(H_0 - V)^2|\psi_{nlm}\rangle$$

$$= -\frac{1}{2m}[E_n^2 - 2E_n\langle\psi_{nlm}|V|\psi_{nlm}\rangle + \langle\psi_{nlm}|V^2|\psi_{nlm}\rangle] \tag{23}$$

For a point-like nucleus the Coulomb potential is given by

$$V = -\frac{Ze^2}{4\pi\varepsilon_0}\frac{1}{r} = -\frac{Z\alpha}{r}$$

where, the fine structure constant is given by

$$\alpha = \frac{e^2}{4\pi\varepsilon_0} = \frac{1}{137}$$

With such potential, Eq. (23) becomes

$$\Delta E_1^{(n)} = -\frac{1}{2m}\left[E_n^2 + 2E_n\left\langle\psi_{nlm}\left|\frac{(Z\alpha)}{r}\right|\psi_{nlm}\right\rangle + \left\langle\psi_{nlm}\left|\frac{(Z\alpha)^2}{r^2}\right|\psi_{nlm}\right\rangle\right] \quad (24)$$

The expectation values of $1/r$ and $1/r^2$ in the Eq. (24) are given by (Sakurai and Napolitano, 2011)

$$\left\langle\psi_{nlm}\left|\frac{Z\alpha}{r}\right|\psi_{nlm}\right\rangle = m(Z\alpha)^2\frac{1}{n^2} = -2E_n, \quad (25)$$

and

$$\left\langle\psi_{nlm}\left|\frac{(Z\alpha)^2}{r^2}\right|\psi_{nlm}\right\rangle = \frac{Z^2\alpha^2}{a_0^2 n^3\left(l+\frac{1}{2}\right)} = 4E_n^2\frac{n}{\left(l+\frac{1}{2}\right)}, \quad (26)$$

where,

$$E_n = -\frac{m(Z\alpha)^2}{2}\frac{1}{n^2} = -\frac{Z^2\alpha}{2a_0}\frac{1}{n^2}, \quad (27)$$

The Bohr's radius a_0 for electronic hydrogen is given by

$$a_0 = \frac{1}{m\alpha}$$

By substituting the result in Eqs. (25) - (27) into Eq. (24) produces

$$\Delta E_1^{(n)} = -\frac{Z^2\alpha E_n}{ma_0}\frac{1}{n^2}\left[\frac{3}{4} - \frac{n}{\left(l+\frac{1}{2}\right)}\right] \quad (28)$$

For $1s_{1/2}$ state, Eq. (28) reduces to

$$\Delta E_1^{(1s_{1/2})} = \frac{5}{4}\frac{Z^2\alpha E_1}{ma_0} \quad (29)$$

Similarly, for $2s_{1/2}$ state Eq. (28) becomes

$$\Delta E_1^{(2s_{1/2})} = \frac{5}{16}\frac{Z^2\alpha E_2}{ma_0},$$

or

$$\Delta E_1^{(2s_{1/2})} = \frac{5}{64}E_1 \quad (30)$$

Note that for muonic hydrogen, the relativistic mass corrections for $1s_{1/2}$ and $2s_{1/2}$ states are obtained from Eqs. (29) and (30) by substituting the Bohr radius a_0 with $a_\mu \backsimeq \frac{1}{207}a_0$.

3.3. Relativistic mass correction for finite size source

Evaluation of the first-order relativistic mass correction for hydrogen-like atoms with Coulomb potential due to a finite size source also starts with Eq. (23). So for the ground state one may write

$$\Delta E_1^{(1s_{1/2})} = -\frac{1}{2m}[E_1^2 - 2E_1\langle\psi_{100}|V|\psi_{100}\rangle + \langle\psi_{100}|V^2|\psi_{100}\rangle] \quad (31)$$

where, $V(r)$ is the potential induced by a uniformly charged spherical nucleus and given by (Adamu and Ngadda, 2017)

$$V(r) = \begin{cases} Z\alpha\left(-\frac{3}{2R} + \frac{r^2}{2R^3}\right), & \text{for } r \le R \\ \frac{-Z\alpha}{r}, & \text{for } r > R \end{cases} \quad (32)$$

By employing this potential, we can evaluate the expectation values of $V(r)$ and $V(r)^2$. Let's start with $\langle V(r)\rangle$ with respect to the $1s_{1/2}$ state. That is

$$\langle\psi_{100}|V|\psi_{100}\rangle = \int\psi_{100}^* V\psi_{100}\mathrm{d}\tau = \int R_{10}^*\,Y_{00}^* V R_{10}Y_{00}\mathrm{d}\tau$$

where,

$$\mathrm{d}\tau = r^2\mathrm{d}r\sin\theta\,\mathrm{d}\theta\mathrm{d}\phi = r^2\mathrm{d}r\mathrm{d}\Omega$$

Let's now rewrite the above integral as

$$\int\psi_{100}^* V\psi_{100}\mathrm{d}\tau = \int R_{10}^*\,VR_{10}r^2\mathrm{d}r\int Y_{00}^*\,Y_{00}\mathrm{d}\Omega \quad (33)$$

The spherical harmonics is normalized, so that the second integral becomes unity (Krane, 988); and hence

$$\int\psi_{100}^* V\psi_{100}\mathrm{d}\tau = \int R_{10}^*\,VR_{10}r^2\mathrm{d}r. \quad (34)$$

In order to evaluate Eq. (24), we partition the integration into two subintervals such that

$$\int\psi_{100}^* V\psi_{100}\mathrm{d}\tau = \int_0^R R_{10}^*\,V_{r\le R}R_{10}r^2\mathrm{d}r + \int_R^\infty R_{10}^*\,V_{r\ge R}R_{10}r^2\mathrm{d}r \quad (35)$$

If we insert Eq. (32) into Eq. (35), then we may obtain

$$\int \psi_{100}^{*} V \psi_{100} \mathrm{d}\tau = Z\alpha \left\{ \int_0^R R_{10}^{*} \left(-\frac{3}{2R} + \frac{r^2}{2R^3} \right) R_{10} r^2 \mathrm{d}r - \int_R^{\infty} R_{10}^{*} \frac{1}{r} R_{10} r^2 \mathrm{d}r \right\} \quad (37)$$

The radial wave function of electronic hydrogen in $1s_{1/2}$ state is given by (Beiser, 2003)

$$R_{10} = \frac{2}{a_0^{3/2}} e^{\frac{-Zr}{a_0}} \quad (38)$$

where, a_0 is the Bohr radius of electronic hydrogen whose value is given by $a_0 = 5.29 \times 10^{-11}\mathrm{m}$. Substituting Eq. (38) into Eq. (37) we obtain

$$\int \psi_{100}^{*} V \psi_{100} \mathrm{d}\tau = \frac{4Z\alpha}{a_0^3} \left\{ \int_0^R \left(\frac{-3}{2R} + \frac{r^2}{2R^3} \right) r^2 e^{\frac{-2Zr}{a_0}} \mathrm{d}r - \int_R^{\infty} r e^{\frac{-2Zr}{a_0}} \mathrm{d}r \right\} \quad (39)$$

We now apply Taylor expansion of the exponential factor in the first term on the right hand side of Eq. (33). Since $r/a_0 \ll 1$, we can approximate as (Arfken, and Weber, 2005)

$$e^{-2Zr/a_0} \cong 1 - \frac{2Zr}{a_0} \quad (40)$$

So that

$$\int \psi_{100}^{*} V \psi_{100} \mathrm{d}\tau = \frac{4Z\alpha}{a_0^3} \left\{ \int_0^R \left(\frac{-3}{2R} + \frac{r^2}{2R^3} \right) \left(1 - \frac{2Zr}{a_0} \right) r^2 \mathrm{d}r - \int_R^{\infty} r e^{\frac{-2Zr}{a_0}} \mathrm{d}r \right\}$$

$$= \frac{4Z\alpha}{a_0^3} \left\{ -\frac{4R^2}{10} - \int_R^{\infty} r e^{\frac{-2Zr}{a_0}} \mathrm{d}r \right\} \quad (41)$$

By using product rule of differentiation we have

$$\mathrm{d}\left(r e^{\frac{-2Zr}{a_0}} \right) = e^{\frac{-2Zr}{a_0}} \mathrm{d}r - \frac{2Z}{a_0} r e^{\frac{-2Zr}{a_0}} \mathrm{d}r$$

Rearranging, we get

$$r e^{\frac{-2Zr}{a_0}} \mathrm{d}r = \frac{a_0}{2Z} e^{\frac{-2Zr}{a_0}} \mathrm{d}r - \frac{a_0}{2Z} \mathrm{d}\left(r e^{\frac{-2Zr}{a_0}} \right) \quad (42)$$

Integrating the above equation, we obtain

$$\int_R^{\infty} r e^{\frac{-2Zr}{a_0}} \mathrm{d}r = -\frac{a_0^2}{4Z^2} e^{\frac{-2Zr}{a_0}} \Big|_R^{\infty} - \frac{a_0}{2Z} r e^{\frac{-2Zr}{a_0}} \Big|_R^{\infty} = \frac{a_0^2}{4Z^2} \left(1 + \frac{2ZR}{a_0} \right) e^{\frac{-2ZR}{a_0}} \quad (43)$$

Substituting Eq. (43) into Eq. (41) we have

$$\int \psi_{100}^{*} V \psi_{100} d\tau = -\frac{8Z\alpha R^2}{5a_0^3} - \frac{\alpha}{Za_0} \left(1 + \frac{2ZR}{a_0} \right) e^{\frac{-2ZR}{a_0}} \quad (44)$$

And also the expectation value of V^2 can be given as

$$\int \psi_{100}^{*} V^2 \psi_{100} \mathrm{d}\tau = \int_0^{\infty} R_{10}^{*} V^2 R_{10} r^2 \mathrm{d}r$$

$$= \int_0^R R_{10}^{*} [V_{r \le R}]^2 R_{10} r^2 \mathrm{d}r + \int_R^{\infty} R_{10}^{*} [V_{r \ge R}]^2 R_{10} r^2 \mathrm{d}r$$

$$= \frac{4(Z\alpha)^2}{a_0^3} \left\{ \int_0^R \left(\frac{9}{4R^2} - \frac{3r^2}{2R^4} + \frac{r^4}{4R^6} \right) r^2 e^{\frac{-2Zr}{a_0}} \mathrm{d}r + \int_R^{\infty} e^{\frac{-2Zr}{a_0}} \mathrm{d}r \right\} \quad (45)$$

Applying the Taylor expansion on the exponential factor in the first integral term of Eq. (45) and then carrying out the integration give rise to

$$\int \psi_{100}^{*} V^2 \psi_{100} \mathrm{d}\tau = \frac{68(Z\alpha)^2 R}{35a_0^3} + \frac{2Z\alpha^2}{a_0^2} e^{\frac{-2ZR}{a_0}} \quad (46)$$

Using Eqs. (44) and (46), Eq. (31) becomes

$$\Delta E_1^{(1s_{1/2})} = -\frac{1}{2m} \left[E_1^2 + \frac{16Z\alpha R^2 E_1}{5a_0^3} + \frac{2E_1\alpha}{Za_0} \left(1 + \frac{2ZR}{a_0} \right) e^{\frac{-2ZR}{a_0}} + \frac{68(Z\alpha)^2 R}{35a_0^3} + \frac{2Z\alpha^2}{a_0^2} e^{\frac{-2ZR}{a_0}} \right]$$

$$= -\frac{1}{2m} \left\{ E_1^2 + \frac{16Z\alpha R^2 E_1}{5a_0^3} + \frac{68(Z\alpha)^2 R}{35a_0^3} + \left[\frac{2E_1\alpha}{Za_0} \left(1 + \frac{2ZR}{a_0} \right) + \frac{2Z\alpha^2}{a_0^2} \right] e^{\frac{-2ZR}{a_0}} \right\} \quad (47)$$

Then for the $1s_{1/2}$ state, the first-order relativistic mass correction for finite size nuclei becomes

$$\Delta E_1^{(1s_{1/2})} = -\frac{1}{2m} \left\{ E_1^2 + \frac{4Z\alpha R(28RE_1 + 17Z\alpha)}{35a_0^3} + \left[\frac{2E_1\alpha}{Za_0} \left(1 + \frac{2ZR}{a_0} \right) + \frac{2Z\alpha^2}{a_0^2} \right] e^{\frac{-2ZR}{a_0}} \right\} \quad (48)$$

Similarly, the first-order relativistic mass correction for the $2s_{1/2}$ state is obtained by rewriting Eq. (31) as

$$\Delta E_1^{(2s_{1/2})} = -\frac{1}{2m} [E_2^2 - 2E_2 \langle \psi_{200} | V | \psi_{200} \rangle + \langle \psi_{200} | V^2 | \psi_{200} \rangle] \quad (49)$$

The expectation values of V and V^2 with respect to the $2s_{1/2}$ state can now be evaluated in what follows. Starting with that of V we have

$$\int \psi_{200}^{*} V \psi_{200} \mathrm{d}\tau = \int_0^{\infty} R_{20}^{*} V R_{20} r^2 \mathrm{d}r$$

$$= \int_0^R R_{20}^* \, V_{r\le R} R_{20} r^2 \mathrm{d}r + \int_R^\infty R_{20}^* \, V_{r\ge R} R_{20} r^2 \mathrm{d}r \qquad (50)$$

where,

$$R_{20} = \frac{1}{2\sqrt{2}a_0^{\frac{3}{2}}}\left(2 - \frac{Zr}{a_0}\right) e^{\frac{-Zr}{2a_0}} \qquad (51)$$

Substituting Eq. (51) into Eq. (50) we obtain

$$\int \psi_{200}^* V \psi_{200} \mathrm{d}\tau = \frac{Z\alpha}{8a_0^3}\left\{\int_0^R V_{r\le R}\left(2 - \frac{Zr}{a_0}\right)^2 e^{\frac{-Zr}{a_0}} r^2 \mathrm{d}r + \int_R^\infty V_{r\ge R}\left(2 - \frac{Zr}{a_0}\right)^2 e^{\frac{-Zr}{a_0}} r^2 \mathrm{d}r\right\} \qquad (52)$$

In the limit $r \ll a_0$, we can employ the binomial expansion for the one of the factors in the first integral becomes

$$\left(2 - \frac{Zr}{a_0}\right)^2 = 4\left(1 - \frac{Zr}{2a_0}\right)^2 \simeq 4\left[1 - \frac{Zr}{2a_0}\right] \qquad (53)$$

Once again, we apply the Taylor expansion to the exponential factor for the first integration and using Eqs. (32) and (53), we have

$$\int \psi_{200}^* V \psi_{200} \mathrm{d}\tau = \frac{Z\alpha}{2a_0^3}\int_0^R \left(-\frac{3r^2}{2R} + \frac{r^4}{2R^3}\right)\mathrm{d}r - \frac{Z\alpha}{8a_0^3}\int_R^\infty \left(4r - \frac{4Zr^2}{a_0} + \frac{Z^2 r^3}{a_0^2}\right) e^{\frac{-Zr}{a_0}} r \mathrm{d}r$$

By following similar steps as in Eqs. (42) and (43) we have

$$\int \psi_{200}^* V \psi_{200} \mathrm{d}\tau = \frac{-Z\alpha R^2}{5a_0^3} - \alpha\left[\frac{1}{4Za_0}\left(1 + \frac{ZR}{a_0}\right) - \frac{ZR^2}{8a_0^3} + \frac{Z^2R^3}{8a_0^4}\right] e^{\frac{-ZR}{a_0}} \qquad (54)$$

and

$$\int \psi_{200}^* V^2 \psi_{200} \mathrm{d}\tau = \int_0^R R_{20}^* \, (V_{r\le R})^2 R_{20} r^2 \mathrm{d}r + \int_R^\infty R_{20}^* \, (V_{r\ge R})^2 R_{20} r^2 \mathrm{d}r$$

$$= \frac{17(Z\alpha)^2 R}{70a_0^3} + \alpha^2\left[\frac{Z}{2a_0^2} - \frac{Z}{4a_0^2}\left(1 + \frac{ZR}{a_0}\right) + \frac{Z^3R^2}{8a_0^4}\right] e^{\frac{-ZR}{a_0}} \qquad (55)$$

Substituting Eqs. (54) and (55) into Eq. (49) we obtain

$$\Delta E_1^{(2s_{1/2})} = -\frac{1}{2m}\left\{E_2^2 + \frac{2\alpha E_2 R^2}{5a_0^3} + \frac{17Z^2\alpha^2 R}{70a_0^3} + \left[\frac{Z\alpha^2}{2a_0^2} + \frac{\alpha E_2}{2Za_0} + \left(\frac{E_2}{2a_0} - \frac{Z^2\alpha}{4a_0^2}\right)\alpha R + \left(\frac{Z^2\alpha}{8a_0^4} - \frac{E_2}{4a_0^3}\right) Z\alpha R^2 + \frac{Z^2\alpha E_2}{4a_0^4} R^3\right] e^{\frac{-ZR}{a_0}}\right\} \qquad (56)$$

In case of muonic hydrogen-like atoms, we may use Eqs. (48) and (56) to estimate the relativistic mass corrections to $1s_{1/2}$ and $2s_{1/2}$ states, respectively, by substituting a_0 with a_μ whose value is given by $a_\mu = 2.56 \times 10^{-13}$ m.

4. Results and Discussion

The corrections in Eqs. (28), (48) and (56) are converted into Matlab source code to produce numerical results. We have used MATLAB software to generate the graph of relativistic mass correction versus proton number. The mass of muon and electron are obtained from CODATA and the nuclear radii for each nucleus is obtained from International Atomic Energy Agency. Table 1 contains the experimental values of important parameters such as rest masses of parti. By employing the experimental values of the parameters given in Table 1, we can estimate the numerical values of first-order relativistic mass correction to $1s_{1/2}$ and $2s_{1/2}$ states for both types of hydrogen-like atoms in the unit of electronvolt (eV).

Table 2 displays those corrections using point-like and finite size charge distributions, separately, for atoms with light and heavy nuclei. It is evident that for electronic hydrogen-like atom, the first-order relativistic mass correction is more prominent in 1s_(1/2) state than 2s_(1/2) state for both types of charge distributions. It was indicated by the authors (Xie et al., 2021) that the relativistic mass correction takes the negative values and decrease continuously. For point-like source, the relativistic mass correction of ground state has been calculated and the result have strong agreement with the present work (Wikipedia, 2022).

Table 1: Experimental values of some parameters used in this numerical analysis.

Nucleus	**Electron mass (MeV)**	**Muon mass (MeV)**	**Bohr Radius of electronic atom ($\mathbf{MeV^{-1}}$)**	**Bohr Radius muonic atom ($\mathbf{MeV^{-1}}$)**	**Nuclear charge Radius ($\mathbf{MeV^{-1}}$)**
	0.5110	105.65836	268.21	1.2975	
$^{1}H_{1}$	–	–	–	–	0.00445
$^{4}He_{2}$	–	–	–	–	0.00997
$^{6}Li_{3}$	–	–	–	–	0.01312
$^{7}Be_{4}$	–	–	–	–	0.01341
$^{12}C_{6}$	–	–	–	–	0.01252
$^{64}Zn_{30}$	–	–	–	–	0.01991

Table 2: The first-order relativistic mass correction for electronic hydrogen-like atoms.

Nucleus	$\Delta E_1^{(1s_{1/2})}$ **with point-like source (eV)**	$\Delta E_1^{(1s_{1/2})}$ **with finite size source (eV)**	$\Delta E_1^{(2s_{1/2})}$ **with point-like source (eV)**	$\Delta E_1^{(2s_{1/2})}$ **with finite size source (eV)**
$^{1}H_{1}$	-9.0569×10^{-4}	-9.0655×10^{-4}	-1.4717×10^{-4}	-1.4772×10^{-4}
$^{3}He_{2}$	-3.6227×10^{-3}	-2.7192×10^{-3}	-5.8870×10^{-4}	-3.5482×10^{-4}
$^{6}Li_{3}$	-8.1551×10^{-3}	-4.2899×10^{-3}	-1.3246×10^{-3}	-5.5065×10^{-4}
$^{7}Be_{4}$	-1.4500×10^{-2}	-5.8000×10^{-3}	-2.3548×10^{-3}	-7.4419×10^{-4}
$^{12}C_{6}$	-3.2605×10^{-2}	-8.7599×10^{-3}	-5.2983×10^{-3}	-1.1314×10^{-3}
$^{64}Zn_{30}$	-8.1511×10^{-1}	-4.3569×10^{-2}	-1.3246×10^{-1}	-7.0491×10^{-3}

Table 3 shows that the corrections due to point-like and finite size charge distributions, separately, for light and heavy nuclei muonic hydrogen. For muonic hydrogen-like atoms, the first-order relativistic mass correction, when considering point-like nuclei, has a better contribution in the $1s_{1/2}$ state than the $2s_{1/2}$ state over the whole range of Z. However, the same cannot be said when taking into account finite size nuclei as the relativistic mass correction is more prominent in $1s_{1/2}$ state than $2s_{1/2}$ state for muonic hydrogen-like atoms with $Z < 15$. But for muonic atoms with heavier nuclei the situation changes in such away that the relativistic mass correction begins to exhibit strong influence over the $2s_{1/2}$ state as compared to the $1s_{1/2}$ state.

Table 3: The first-order relativistic mass correction for muonic hydrogen-like atoms.

Nucleus	$\Delta E_1^{(1s_{1/2})}$ **with point-like source (eV)**	$\Delta E_1^{(1s_{1/2})}$ **with finite size source (eV)**	$\Delta E_1^{(2s_{1/2})}$ **with point-like source (eV)**	$\Delta E_1^{(2s_{1/2})}$ **with finite size source (eV)**
$^{1}H_{1}$	-1.8736×10^{-1}	-1.8609×10^{-1}	-3.0447×10^{-2}	-4.7251×10^{-2}
$^{3}He_{2}$	-7.4946×10^{-1}	-5.5244×10^{-1}	-1.2179×10^{-1}	-2.2342×10^{-1}
$^{6}Li_{3}$	-1.68630×10^{0}	-8.5973×10^{-1}	-1.9673×10^{-1}	-5.5836×10^{-1}
$^{7}Be_{4}$	-2.99783×10^{0}	-1.15121×10^{0}	-4.8715×10^{-1}	-9.6176×10^{-1}
$^{12}C_{6}$	-6.74512×10^{0}	-1.71430×10^{0}	-1.09610×10^{0}	-1.93145×10^{0}
$^{64}Zn_{30}$	-1.68640×10^{2}	-7.62900×10^{0}	-2.74020×10^{1}	-6.92000×10^{1}

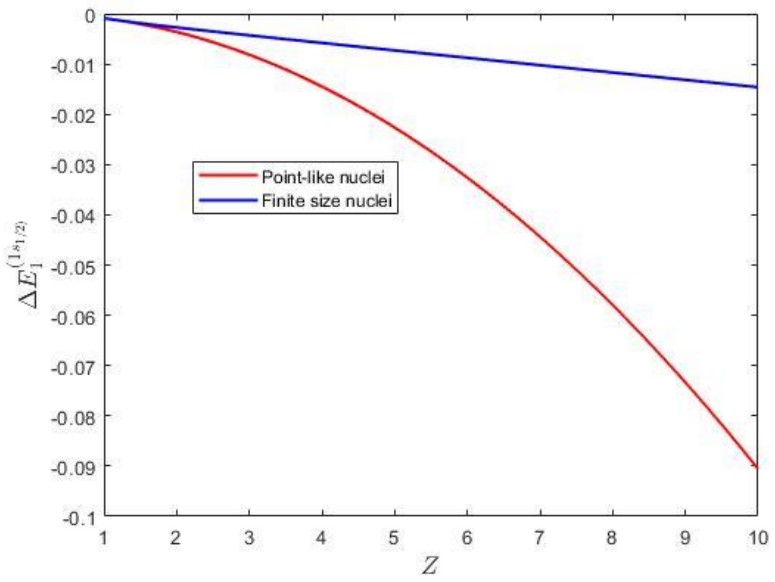

Figure 1: Relativistic mass correction versus proton number for $1s_{1/2}$ state electronic atom.

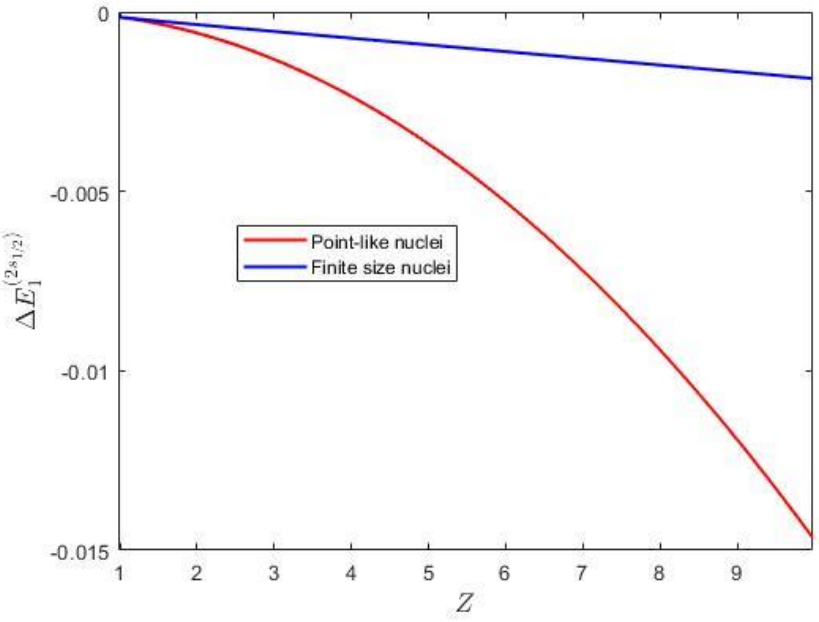

Figure 2: Relativistic mass correction versus proton number for $2s_{1/2}$ sate electronic atom.

Figures 1 and 2 depict that the results of both present work (finite size source) and point-like source for electronic hydrogen atom. The results show that as the atomic number (Z) increases, the relativistic mass corrections decrease for the two types of hydrogen-like atoms. The plots also clearly indicate that the correction with finite size charge distribution agrees with that of the point-like source in case of hydrogen-like atoms with light nuclei. Nevertheless, as Z increases, there is strong deviation of the corrections with finite size distributions from the ones with point-like sources.

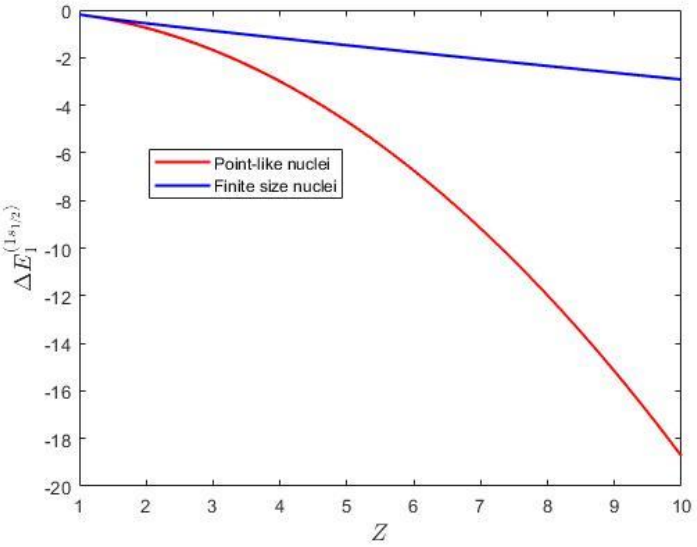

Figure 3: Relativistic mass correction versus proton number for $1s_{1/2}$ state muonic atom.

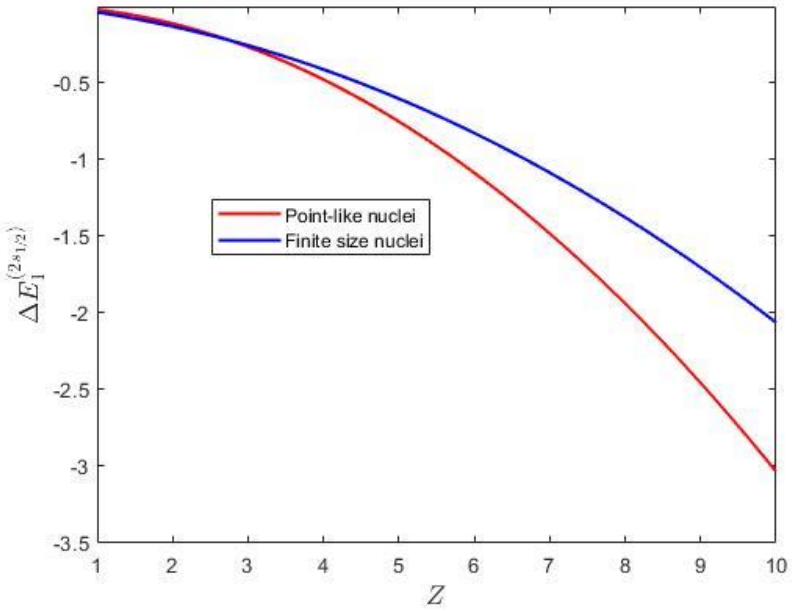

Figure 4: Relativistic mass correction versus proton number for $2s_{1/2}$ state muonic atom.

Figures 3 and 4 illustrate the dependence of the relativistic mass correction on the proton number Z for $1s_{1/2}$ and $2s_{1/2}$ states of muonic hydrogen-like atoms. According to Figure 3, as the atomic number increases so is the deviation of the relativistic mass correction to $1s_{1/2}$ state with finite size nuclei from the one with point-like charge distribution. Based on Figure 4 the relativistic mass corrections to $2s_{1/2}$ state of muonic hydrogen-like atoms with finite size and point-like nuclei show slightly better agreement as opposed to the case of the $1s_{1/2}$ states of similar atoms.

5. Conclusion

In this paper, we have shown how, in non-relativistic limit, Dirac equation can be reduced into Schrodinger equation and we have presented the mathematical approach used to calculate the relativistic mass correction by using potentials from point-like and finite size source charge distributions. The results show that, for hydrogen-like atoms with light nuclei the relativistic mass corrections due to the finite size source roughly coincides with that of point-like source. However, for atoms with heavy nuclei the two corrections display

strong disagreement in which the corrections with finite size nuclei are significantly smaller than that of point-like nuclei.

Declarations

Competing interests: The authors declare that they have no competing interests.

Reference

Adamu, A., & Ngadda, Y. H. (2017). Determination of Nuclear Potential Radii and Its Parameter from Finite–Size Nuclear Model. *International Journal of Theoretical and Mathematical Physics*, 7: 9-13.

Adamu, A., Hassan, M., Dikwa, M. K., & Amshi, S. A. (2018). Determination of Nuclear Structure Effects on Atomic Spectra by Applying Rayleigh–Schrödinger Perturbation Theory. *American Journal of Quantum Chemistry and Molecular Spectroscopy*, 2: 39-51.

Arfken, G. B. and Weber, H. J. (2005). *Mathematical Methods for Physicists*. 6th Edition, Elsevier Inc.

Beiser, A. (2003). *Concepts of Modern Physics*. 6th edition. McGraw-Hill, New York.

Deck, R. T., Amar, J. G., Fralick, .G. (2005). Nuclear size corrections to the energy levels of single-electron and -muon atoms. *Journal of Physics B Atomic Molecular and Optical Physics*, 38(13): 2173—2186.

Deur, A. (2021). Relativistic corrections to the rotation curves of disk galaxies. *The European Physical Journal C*, 81(3): 1-10.

Eshetu Diriba Kena & Gashaw Bekele Adera. (2021). Solving the Dirac equation in central potential for muonic hydrogen atom with point-like nucleus. *Journal of Physics Communications*, 5(10): 105018.

Firew, M. (2020). Investigating Muonic Hydrogen Atom Energy Spectrum Using Perturbation Theory in Lowest Order. Adv. Phys. App. 83.

Griffiths, J. D., (1995). *Introduction to Quantum mechanics*. 2nd edition, Prentice Hall, Inc., New Jersey, USA.

Hudson, A., Nelson, R. (1990). University physics Volume Two, 2nd edition.

Iliaš, M., Kellö, V., & Urban, M. (2010). Relativistic effects in atomic and molecular properties. *Acta Phys. Slovaca*, 60(3): 259-391.

International Atomic Energy Agency. (2022). Nuclear Data Services. https://www-nds.iaea.org/radii/

Krane, K.S. (1988). *Introductory Nuclear Physics*. John Wiley & Sons. New York.

Maggiore, M. (2005). A Modern Introduction to Quantum Field Theory. Oxford University Press.

Messiah A. (1966). Quantum Mechanics Volume II (New York: John Wiley and sons Inc.)

Niri, B. N., Anjami, A. (2018). Nuclear Size Corrections to the Energy Levels of Single-Electron Atoms. *Nuclear Science*, 3(1): 1-8.

Patoary, A. S. M., & Oreshkina, N. S. (2018). Fnite nuclear size effect to the fine structure of heavy muonic atoms. *The European Physical Journal D*, 72(3): 1-4.

Pohl, R. (2014). The Lamb shift in muonic hydrogen and the proton radius puzzle. *Hyperfine Interactions*, 227 (1-3): 23-28.

Pohl, R. Gilman, R., Miller, G. A., Pachucki. (2013). Muonic Hydrogen and the Proton Radius Puzzle. *Annual Review of Nuclear and Particle Science*, 63 (1).

Pyper, N. C. (2020). Relativity and the periodic table. *Philosophical Transactions of the Royal Society A*, 378(2180), 20190305.

Sakurai, J.J. and Napolitano, J. (2011). *Modern Quantum Mechanics*. 2nd edition, Addison-Wesley.

Schwabl, F. (2008). *Advanced Quantum Mechanics*. 4th edition, Springer-Verlag Berlin Heidelberg.

Townsend, J.S. (2012). *A modem approach to quantum mechanics*, 2nd edition.

Wikipedia. (2022). https://en.wikipedia.org/wiki/Fine_structure

Xie, H. H., Jiao, L. G., Liu, A., & Ho, Y. K. (2021). High-precision calculation of relativistic corrections for hydrogen-like atoms with screened Coulomb potentials. *International Journal of Quantum Chemistry*, 121(13): e26653.